Vietnam Journal of Mechanics, Vol. 46, No. 1 (2024), pp. 31 – 43
DOI: https://doi.org/10.15625/0866-7136/20579

VIBRATION ANALYSIS OF TIMOSHENKO MICROBEAMS MADE OF FUNCTIONALLY GRADED MATERIALS ON A WINKLER–PASTERNAK ELASTIC FOUNDATION

Tran Van Lien[1], **Le Thi Ha**[2,*]
[1]*Hanoi University of Civil Engineering, Hanoi, Vietnam*
[2]*University of Transport and Communications, Hanoi, Vietnam*
E-mail: lethiha@utc.edu.vn

Received: 21 January 2024 / Revised: 19 March 2024 / Accepted: 22 March 2024
Published online: 31 March 2024

Abstract. In this work, the free vibration analysis of Timoshenko microbeams made of the Functionally Graded Material (FGM) on the Winkler–Paternak elastic foundation based on the Modified Coupled Stress Theory (MCST) is investigated. Material characteristics of the beam vary throughout the thickness according to the power distribution and are estimated though Mori–Tanaka, Hashin–Shtrikman and Voigt homogenization techniques. The Timoshenko microbeam model considering the length scale parameter is applied. The free vibration differential equations of FGM microbeams are established based on the Finite Element Method (FEM) and Kosmatka's shape functions. The influences of the size-effect, foundation, material, and geometry parameters on the vibration frequency are then analyzed. It is shown that the study can be applied to other FGMs as well as more complex beam structures.

Keywords: FGM, microbeam, nondimensional frequency, MCST.

1. INTRODUCTION

Functionally Graded Materials (FGMs) are inhomogeneous composites which have attracted considerable attention due to their novel thermo-mechanical properties that enable them to be used in a wide range of applications in many industries such as aircrafts, biomedical products, space vehicles... Micro–Electro-Mechanical Systems (MEMS) are the new field in which FGMs have been utilized to achieve the desired performance. Micro-sized structures as plates, sheets, beams, and framed structures are widely used in MEMS devices, for example, electrically actuated micro electromechanical devices,

atomic force microscopes... For this reason, microstructures made of FGMs are especially attracting more and more attention due to their various potential applications.

The classical mechanical theories fail to satisfy the solution of the micro elements because it is not effort the size-effect in the micro-scale. So, the non-classical theories such as Modified Couple Stress Theory (MCST) [1] and Modified Strain Gradient Theory (MSGT) [2] must be used in the mechanics of the micro structures which effort the size-effect in the microstructure.

Simsek and Reddy [3, 4] examined static bending and free vibration of FGM microbeams based on the MCST and various higher order beam theories. Ansari et al. [5] investigated free vibration characteristics of FGM microbeams based on the MSGT and the Timoshenko beam theory (TBT). Kahrobaiyan et al. [6] developed a new comprehensive microbeam element on the basis of the MCST. The shape functions of the new element are derived by solving the governing equations of MCST homogeneous Timoshenko beams. Using the differential quadrature method, Ke and Wang [7] investigated the dynamic stability of FGM microbeams based on the MCST and the TBT. The material properties of FGM microbeams are assumed to vary in thickness direction and are estimated though Mori–Tanaka homogenization technique. Thai et al. [8] examined static bending, buckling and free vibration behaviors of size-dependent FGM sandwich microbeams based on the MCST and the TBT. To avoid the use of a shear correction factor, equilibrium equations were used to compute the transverse shear force and shear stress. Using third-order shear deformation theory, Salamat-Talab et al. [9] investigated the static and dynamic analysis of the FGM microbeam based on the MCST. By the Rayleigh–Ritz method, Akgöz and Civalek [10] studied vibration responses of non-homogenous and non-uniform microbeams using the Bernoulli–Euler beam theory (EBT) and the MCST. The boundary conditions of the microbeam are considered as fixed at one end and free at the other end. It is taken into consideration that material properties and the cross section of the microbeam vary continuously along the longitudinal direction. Chen et al. [11] investigated the static and dynamic responses of bi-directional functionally graded microbeams. The material properties vary along both thickness and axial directions. Shafiei et al. [12] investigated the size dependent nonlinear vibration behavior of imperfect uniform and non-uniform FGM microbeams based on the MCST and the EBT.

In this work, free vibration of FGM microbeams on a Winkler–Pasternak elastic foundation is studied based on the MCST, the TBT and the Mori–Tanaka, Hashin–Shtrikman and Voigt homogenization techniques. The governing equations of vibration for the TBT microbeam are derived by using the Finite Element Method (FEM) and Kosmatka's shape functions. A detailed study is performed to investigate the influences of material, foundation parameter, dimensionless length scale parameter and slenderness ratio on the natural frequencies of FGM microbeams.

2. PROBLEM AND FORMULATION

Consider an FGM microbeam of the length L and rectangular cross-section $b \times h$ on the Winkler-Pasternak elastic foundation as shown in Fig. 1. It is assumed that the materials at bottom surface ($z = h/2$) and top surface ($z = h/2$) of the microbeam are metals and ceramics, respectively. The local effective material properties of the FGM microbeam can be calculated using the Mori–Tanaka, Hashin-Shtrikman and Voigt homogenization techniques.

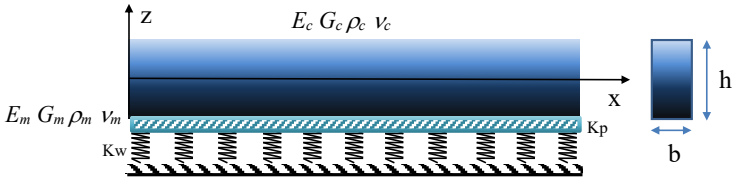

Fig. 1. A FGM microbeam on a Winkler-Pasternak elastic foundation

According to the Mori–Tanaka homogenization technique [13], the effective bulk modulus K and shear modulus G can be calculated by

$$\begin{aligned} \frac{K-K_m}{K_c-K_m} &= \frac{V_c}{1+(1-V_c)(K_c-K_m)/(K_m+4G_m/3)}, \\ \frac{G-G_m}{G_c-G_m} &= \frac{V_c}{1+\dfrac{(1-V_c)(G_c-G_m)}{G_m+G_m\left(9K_m+8G_m\right)/\left(6K_m+12G_m\right)}}, \end{aligned} \tag{1}$$

where the subscripts m and c denote metal and ceramic materials, respectively; V denotes the volume fraction of the phase materials. The variation of the volume fraction of constituents can be described by a power function as follows

$$V_c = \left(\frac{1}{2}+\frac{z}{h}\right)^n, \quad V_m = 1-\left(\frac{1}{2}+\frac{z}{h}\right)^n, \tag{2}$$

where n is the volume fraction index. Effective material properties of the FGM microbeam such as Young's modulus E, Poisson's ratio ν, shear modulus G and mass density ρ can be determined as follows

$$E(z) = \frac{9KG}{3K+G}, \quad \nu(z) = \frac{3K-2G}{2(3K+G)}, \quad G(z) = \frac{E\left(z\right)}{2(1+\nu(z))}, \quad \rho(z) = \rho_c V_c + \rho_m V_m, \tag{3}$$

Hashin–Shtrikman have evaluated the effective bulk modulus K and shear modulus G as follows

$$K = K_c + \frac{V_m}{\dfrac{1}{K_m-K_c}+\dfrac{1-V_m}{K_c+G_c}}, \quad G = G_c + \frac{V_m}{\dfrac{1}{G_m-G_c}+\dfrac{(1-V_m)\left(K_c+2G_c\right)}{2G_c(K_c+G_c)}}. \tag{4}$$

The Voigt estimate is a frequently used estimate effective material properties P such as E, G, ρ based on the case of a two-phase composite because of the simplicity of this estimate

$$P = P_m V_m(z) + P_c V_c(z). \tag{5}$$

The displacements at a point on the cross-section of the Timoshenko beam can be represented as

$$u(x,z,t) = u_0(x,t) - (z-h_0)\theta(x,t), \quad w(x,z,t) = w_0(x,t), \tag{6}$$

where $u_0(x,t), w_0(x,t)$ are the axial displacement, the deflection of a point on axis, respectively; θ is the angle of rotation of the cross-section around the y axis; h_0 is the distance from the neutral axis to x-axis. The nonzero deformation and stress components using the MCST are obtained as follows

$$\begin{aligned}
&\varepsilon_{xx} = \frac{\partial u_0}{\partial x} - (z-h_0)\frac{\partial \theta}{\partial x}, \quad \varepsilon_{xz} = \frac{\gamma_{xz}}{2} = \frac{1}{2}\left(\frac{\partial w_0}{\partial x} - \theta\right),\\
&\sigma_{xx} = (\lambda + 2G)\left[\frac{\partial u_0}{\partial x} - (z-h_0)\frac{\partial \theta}{\partial x}\right], \quad \sigma_{xz} = G\left(\frac{\partial w_0}{\partial x} - \theta\right), \quad \sigma_{yy} = \sigma_{zz} = \lambda \varepsilon_{xx},\\
&\chi_{xy} = -\frac{1}{4}\left(\frac{\partial^2 w_0}{\partial x^2} + \frac{\partial \theta}{\partial x}\right), \quad m_{xy} = -\frac{1}{2}Gl^2\left(\frac{\partial^2 w_0}{\partial x^2} + \frac{\partial \theta}{\partial x}\right),
\end{aligned} \tag{7}$$

where λ, G are the Lame's coefficient and shear modulus determined from E and ν as follows

$$\lambda(z) = \frac{\nu(z)E(z)}{[1+\nu(z)][1-2\nu(z)]}, \quad G(z) = \frac{E(z)}{2[1+2\nu(z)]}, \tag{8}$$

l is the scale material parameter, and m_{xy}, χ_{xy} are components of the deviatoric couple stress $\mathbf{m}$ and curvature $\boldsymbol{\chi}$ tensors, respectively.

The strain energy U of the microbeam

$$\begin{aligned}
U &= \frac{1}{2}\int_0^L \int_A \left(\sigma_{xx}\varepsilon_{xx} + 2k_s\sigma_{xz}\varepsilon_{xz} + 2m_{xy}\chi_{xy}\right)\mathrm{d}A\mathrm{d}x\\
&= \frac{1}{2}\int_0^L \left\{\left[A_{11}\left(\frac{\partial u_0}{\partial x}\right)^2 - 2A_{12}\frac{\partial u_0}{\partial x}\frac{\partial \theta}{\partial x} + A_{22}\left(\frac{\partial \theta}{\partial x}\right)^2\right]\right.\\
&\quad \left. + k_s A_{33}\left(\frac{\partial w_0}{\partial x} - \theta\right)^2 + \frac{1}{4}l^2 A_{33}\left(\frac{\partial^2 w_0}{\partial x^2} + \frac{\partial \theta}{\partial x}\right)^2\right\}\mathrm{d}x,
\end{aligned} \tag{9}$$

where k_s is the shear correction factor and

$$(A_{11}, A_{12}, A_{22}) = \int_A [\lambda(z) + 2G(z)]\left(1, z, z^2\right)\mathrm{d}A, \quad A_{33} = \int_A G(z)\mathrm{d}A, \tag{10}$$

A_{11}, A_{12}, A_{22} and A_{33} are the rigidities. The kinetic energy T of the microbeam is then given by

$$\begin{aligned} T &= \frac{1}{2}\int_0^L \int_A \rho\,(z)\left\{\left(\frac{\partial u}{\partial t}\right)^2 + \left(\frac{\partial w}{\partial t}\right)^2\right\}\mathrm{d}A\mathrm{d}x \\ &= \frac{1}{2}\int_0^L \left\{ I_{11}\left[\left(\frac{\partial u_0}{\partial t}\right)^2 + \left(\frac{\partial w_0}{\partial t}\right)^2\right] - I_{12}\left(\frac{\partial u_0}{\partial t}\frac{\partial \theta}{\partial t} + \frac{\partial \theta}{\partial t}\frac{\partial u_0}{\partial t}\right) + I_{22}\left(\frac{\partial \theta}{\partial t}\right)^2\right\}\mathrm{d}x, \end{aligned} \tag{11}$$

where I_{11}, I_{12} and I_{22} are the mass moments

$$(I_{11}, I_{12}, I_{22}) = \int_A \rho(z)\left(1, z, z^2\right)\mathrm{d}A. \tag{12}$$

The strain energy U_F of the Winkler–Pasternak foundation

$$U_F = \frac{1}{2}\int_0^L \left[K_w \mathbf{w}^2 + K_p\left(\frac{\mathrm{d}\mathbf{w}}{\mathrm{d}x}\right)^2\right]\mathrm{d}x, \tag{13}$$

where K_w and K_p define the spring and shear moduli of the Winkler–Pasternak elastic foundation.

Using the FEM, the beam is assumed to be divided into numbers of two-node beam elements of length L. The vector of nodal displacements $\mathbf{d}_e$ for the element considering the transverse shear rotation θ as an independent variable contains six components as

$$\mathbf{d}_e = \left\{u_i, w_i, \theta_i, u_j, w_j, \theta_j\right\}^T, \tag{14}$$

where $u_i, w_i, \theta_i, u_j, w_j, \theta_j$ are the values of u_0, w_0 and θ at the node i and at the node j, respectively. In Eq. (14) and hereafter, a superscript 'T' is used to denote the transpose of a vector or a matrix.

$$\begin{Bmatrix} u_0 \\ w_0 \\ \theta \end{Bmatrix} = \begin{bmatrix} N_1^u & 0 & 0 & N_2^u & 0 & 0 \\ 0 & N_1^w & N_2^w & 0 & N_3^w & N_4^w \\ 0 & N_1^\theta & N_2^\theta & 0 & N_3^\theta & N_4^\theta \end{bmatrix} \begin{Bmatrix} u_i & w_i & \theta_i & u_j & w_j & \theta_j \end{Bmatrix}^T = \begin{bmatrix} \mathbf{N}^u \\ \mathbf{N}^w \\ \mathbf{N}^\theta \end{bmatrix} \mathbf{d}_e, \tag{15}$$

where $\mathbf{N}^u$ is the Lagrange's linear shape function, $\mathbf{N}^w$ and $\mathbf{N}^\theta$ are Kosmatka's shape functions [14]

$$
\begin{aligned}
&N_1^u = 1 - x/L, \quad N_2^u = x/L,\\
&N_1^w = 1 + \frac{1}{1+\varphi}\left[2\left(\frac{x}{L}\right)^3 - 3\left(\frac{x}{L}\right)^2 - \varphi\left(\frac{x}{L}\right)\right],\\
&N_2^w = \frac{L}{2(1+\varphi)}\left[2\left(\frac{x}{L}\right)^3 - (4+\varphi)\left(\frac{x}{L}\right)^2 + (2+\varphi)\left(\frac{x}{L}\right)\right],\\
&N_3^w = \frac{-1}{1+\varphi}\left[2\left(\frac{x}{L}\right)^3 - 3\left(\frac{x}{L}\right)^2 - \varphi\left(\frac{x}{L}\right)\right],\\
&N_4^w = \frac{L}{2(1+\varphi)}\left[2\left(\frac{x}{L}\right)^3 + (\varphi-2)\left(\frac{x}{L}\right)^2 - \varphi\left(\frac{x}{L}\right)\right],\\
&N_1^\theta = -\frac{6}{L(1+\varphi)}\left(\frac{x}{L}\right)\left(1-\frac{x}{L}\right), \quad N_2^\theta = \left(1-\frac{x}{L}\right)\left[1 - \frac{3}{(1+\varphi)}\left(\frac{x}{L}\right)\right],\\
&N_3^\theta = \frac{6}{L(1+\varphi)}\left(\frac{x}{L}\right)\left(1-\frac{x}{L}\right), \quad N_4^\theta = \left(\frac{x}{L}\right)\left[1 - \frac{3}{(1+\varphi)}\left(1-\frac{x}{L}\right)\right],
\end{aligned}
\tag{16}
$$

and

$$
\varphi = \frac{12A_{22}}{k_s A_{33} L^2}. \tag{17}
$$

The element stiffness and mass matrices of the microbeam element are obtained as follows

$$
\mathbf{k}_{e,b} = \int_0^L \mathbf{B}_e^T \mathbf{D}_e \mathbf{B}_e \mathrm{d}x, \quad \mathbf{m}_e = \int_0^L \begin{pmatrix} \mathbf{N}^u \\ \mathbf{N}^w \\ \mathbf{N}^\theta \end{pmatrix}^T \begin{bmatrix} \rho A & 0 & 0 \\ 0 & \rho A & 0 \\ 0 & 0 & \rho I \end{bmatrix} \begin{pmatrix} \mathbf{N}^u \\ \mathbf{N}^w \\ \mathbf{N}^\theta \end{pmatrix} \mathrm{d}x, \tag{18}
$$

where

$$
\mathbf{B}_e = \begin{bmatrix} \dfrac{\partial \mathbf{N}^u}{\partial x} \\ \dfrac{\partial \mathbf{N}^\theta}{\partial x} \\ \dfrac{\partial \mathbf{N}^w}{\partial x} - \mathbf{N}^\theta \\ \dfrac{1}{4}\left(\dfrac{\partial^2 \mathbf{N}^w}{\partial x^2} + \dfrac{\partial \mathbf{N}^\theta}{\partial x}\right) \end{bmatrix}, \quad \mathbf{D}_e = \begin{bmatrix} EA & 0 & 0 & 0 \\ 0 & EI & 0 & 0 \\ 0 & 0 & k_s GA & 0 \\ 0 & 0 & 0 & 4GAl^2 \end{bmatrix}. \tag{19}
$$

The stiffness matrices of the Winkler–Pasternak elastic foundation are obtained as follows

$$\begin{aligned}\mathbf{k}_{e,w} &= \frac{1}{2}\int_0^{L_e} K_w \left(\mathbf{N}^w\right)^T \mathbf{N}^w \mathrm{d}x,\\ \mathbf{k}_{e,p} &= \frac{1}{2}\int_0^{L_e} K_p \left(\frac{\partial \mathbf{N}^w}{\partial x}\right)^T \frac{\partial \mathbf{N}^w}{\partial x}\mathrm{d}x.\end{aligned} \tag{20}$$

Having the element stiffness and mass matrices derived, the equations of motion for the free vibration analysis can be written in the form

$$\mathbf{M}\ddot{\mathbf{D}} + \mathbf{K}\mathbf{D} = \mathbf{0}, \tag{21}$$

where **D**, **M**, and **K** are the structural nodal displacement vector, mass and stiffness matrices obtained by assembling the element displacement vector $\mathbf{d}_e$, the mass matrix $\mathbf{m}_e$, and stiffness matrices $\mathbf{k}_e$, $\mathbf{k}_{ew}$ and $\mathbf{k}_{ep}$ over the total elements, respectively.

3. NUMERICAL RESULT AND DISCUSSION

In this section, the free vibration of the FGM microbeam on the elastic foundation is studied. It is considered the FGM microbeams consist of the aluminum (Al) and the ceramic (SiC) with the material properties $E_m = 70$ GP, $\nu_m = 0.3$, $\rho_m = 2702$ kg/m^3 for Al and $E_c = 427$ GP, $\nu_c = 0.17$, $\rho_c = 3100$ kg/m^3 for SiC. The material scale parameter is equal to $l = 15$ μm. The nondimensional frequencies μ_i are defined as follows

$$\mu_i = \frac{\omega_i L^2}{h}\sqrt{\frac{\rho_m}{E_m}}. \tag{22}$$

The Winkler–Paternak foundation coefficients are given in the nondimensional form

$$k_w = \frac{K_w L^4}{E_m I}, \quad k_p = \frac{K_p L^2}{E_m I}, \quad I = \frac{bh^3}{12}. \tag{23}$$

To validate the proposed FEM model, the results obtained from the present analysis are compared with the analytical solutions given by Ansari et al. [5]. In Table 1, the nondimensional fundamental frequencies of the simply supported microbeam with an aspect ratio $L/h = 10$ and the volume fraction index $n = 2$ obtained in the present paper are compared with the results by Ansari et al. A good agreement can be received for the different material length scale parameters. The above comparisons validate the reliability of the proposed FEM model.

Table 1. Comparison of fundamental frequency parameters for FGM microbeams ($L/h = 10, n = 2$)

h (μm)	15	30	45	60	75	90
Ansari et al.	0.7983	0.5100	0.4341	0.4041	0.3894	0.3811
Present (M)	0.7655	0.5062	0.4349	0.4064	0.3924	0.3845
Present (H)	0.7976	0.5213	0.4444	0.4135	0.3983	0.3897

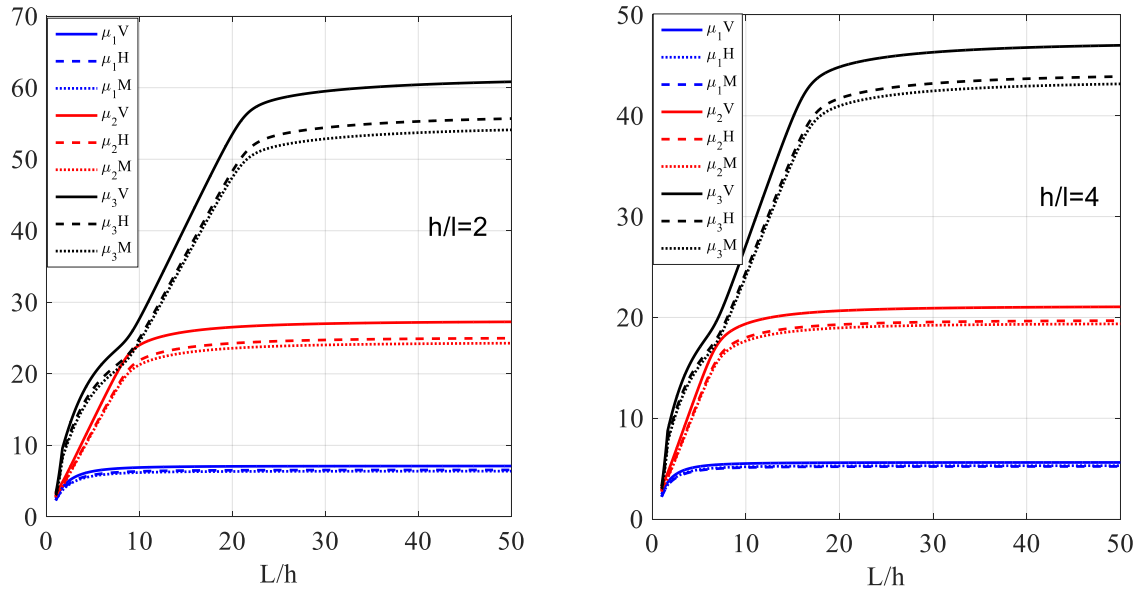

(a) $h/l = 2$ (b) $h/l = 4$

Fig. 2. Effects of the L/h ratios on the first three nondimensional frequencies of the FGM microbeams when $k_w = 50, k_p = 30, n = 2$ using homogenization techniques Voigt (V), Hashin–Shtrikman (H) and Mori–Tanaka (M) and different ratios h/l

Fig. 2 shows the variation of the first three nondimensional frequencies of the FGM microbeams with Winkler–Paternak foundation coefficients $k_w = 50$, $k_p = 30$ and the volume fraction index $n = 2$ using homogenization techniques Voigt (V), Hashin–Shtrikman (H), Mori–Tanaka (M) and different ratios $h/l = 2$ (Fig. 2(a)), $h/l = 4$ (Fig. 2(b)). It shows that nondimensional frequencies using the Hashin-Shtrikman homogenization technique are a little higher than nondimensional frequencies using the Mori–Tanaka homogenization technique, but both of them are smaller than nondimensional frequencies using the Voigt homogenization technique, specially for the higher frequencies. Moreover, nondimensional frequencies using three homogenization techniques increase when the ratio L/h increases. However, "turning point" ratios L/h, at which the given nondimensional

frequency changes from the increase to the constant, are dependent on the given frequency and the ratios h/l: the higher the frequency the higher the "turning point" ratio L/h, the lower the ratio h/l the higher the "turning point" ratio L/h.

Fig. 3 shows the effects of the slenderness ratio h/l on the first three nondimensional frequency of FGM microbeams with Winkler–Paternak foundation coefficients k_w = 50, k_p = 30 and the volume fraction index n = 5 using homogenization techniques Voigt (V), Hashin–Shtrikman (H), Mori–Tanaka (M) and different ratios $L/h = 10$ (Fig. 3(a)), $L/h =$ 50 (Fig. 3(b)). It can be seen that first three nondimensional frequencies decrease when the ratios h/l increase. Moreover, the difference of the second frequency and the third frequency are remarkable when the ratio L/h and h/l are higher.

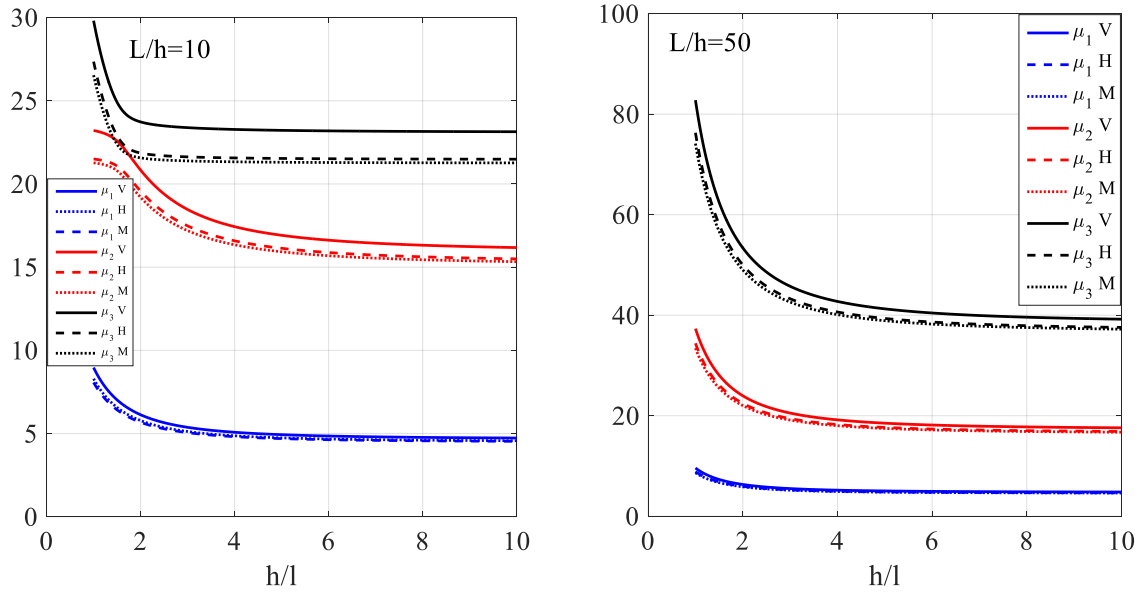

(a) $L/h = 10$ (b) $L/h = 50$

Fig. 3. Effects of the slenderness ratios h/l on the first three nondimensional frequencies of the FGM microbeams when $k_w = 50, k_p = 30, n = 5$ using homogenization techniques Voigt (V), Hashin–Shtrikman (H) and Mori–Tanaka (M) and different ratios L/h

Fig. 4 shows the effects of the volume fraction index n on first three nondimensional frequencies of FGM microbeams with Winkler–Paternak foundation coefficients k_w = 50, k_p = 30, h/l = 2 using homogenization techniques Voigt (V), Hashin–Shtrikman (H), Mori–Tanaka (M) and different ratios L/h: a) $L/h = 10$; b) $L/h = 50$. It can be seen that first three nondimensional frequencies decrease when the volume fraction index n increases. Moreover, the difference between the second frequency and the third frequency are remarkable when the ratio L/h and the volume fraction index n are higher.

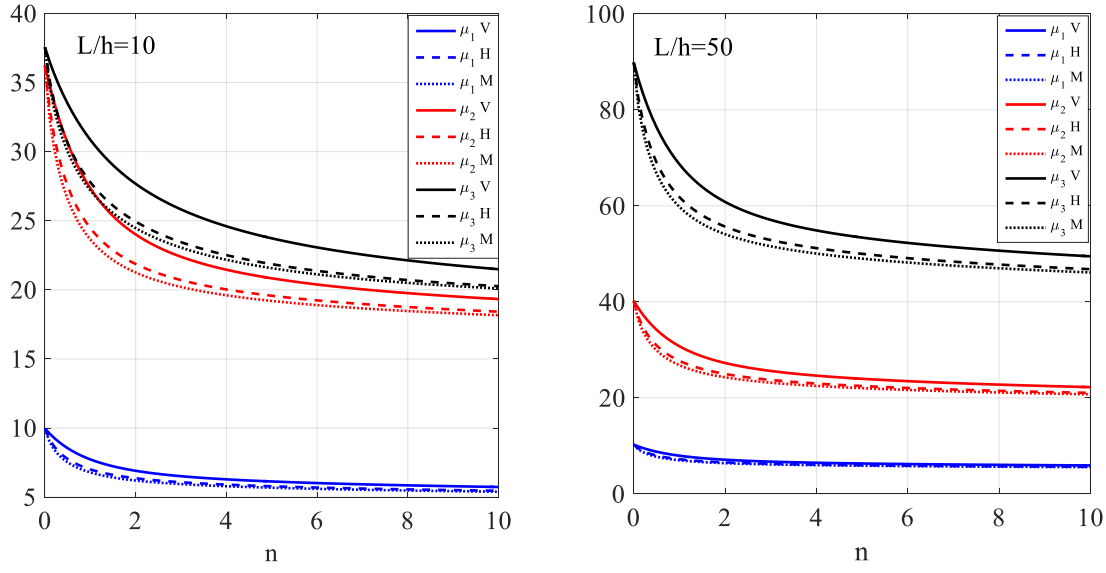

(a) $L/h = 10$ (b) $L/h = 50$

Fig. 4. Effects of the volume fraction index n on the first three nondimensional frequencies of the FGM microbeams when $k_w = 50, k_p = 30, h/l = 2$ using homogenization techniques Voigt (V), Hashin–Shtrikman (H) and Mori–Tanaka (M) and different ratios L/h

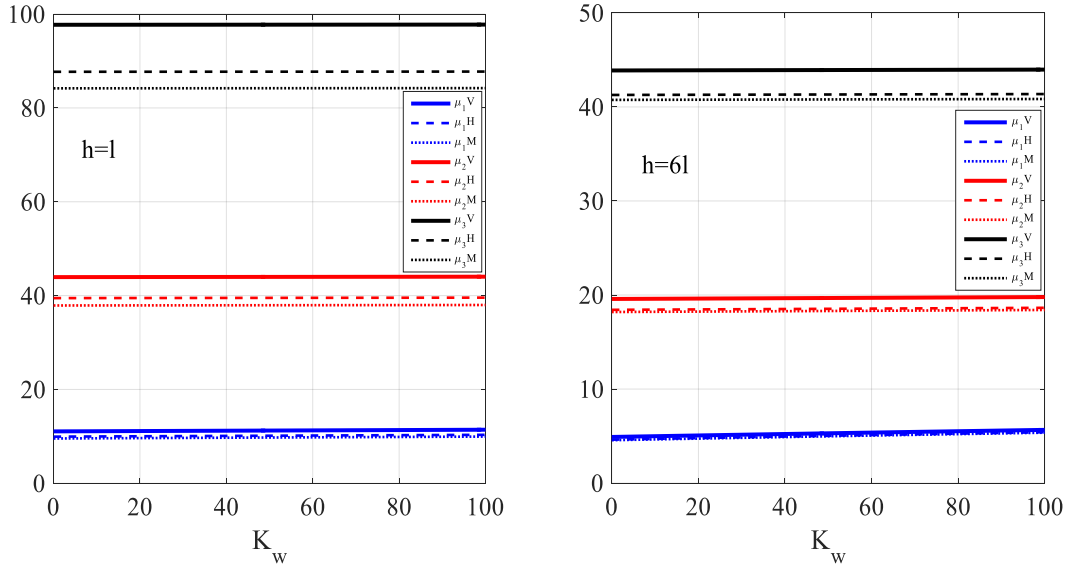

(a) $h/l = 1$ (b) $h/l = 6$

Fig. 5. Effects of the Winkler foundation coefficients k_w on the first three nondimensional frequencies of the FGM microbeams when $k_p = 20, n = 2, L/h = 10$ using homogenization techniques Voigt (V), Hashin–Shtrikman (H) and Mori–Tanaka (M) and different ratios h/l

Fig. 5 shows the effects of the Winkler elastic foundation coefficient k_w on first three nondimensional frequencies of FGM microbeams with Paternak foundation coefficients $k_p = 30$, $n = 2$ and $L/h = 10$ using homogenization techniques Voigt (V), Hashin–Shtrikman (H), Mori–Tanaka (M) and different ratios $h/l = 1$ (Fig. 5(a)), $h/l = 6$ (Fig. 5(b)). It can be seen that the value of the first three nondimensional frequencies increase unremarkably, especially when the ratio h/l is small.

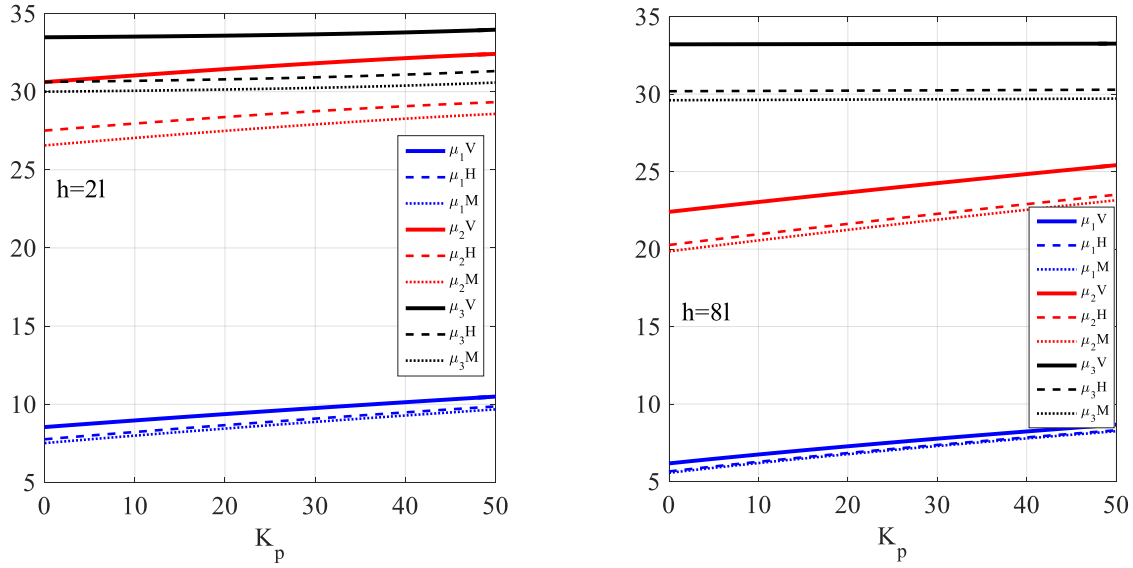

(a) $h/l = 2$ (b) $h/l = 8$

Fig. 6. Effects of the Paternak foundation coefficients k_p on the first three nondimensional frequencies of the FGM microbeams with $k_w = 20, n = 0.5, L/h = 10$ and using homogenization techniques Voigt (V), Hashin–Shtrikman (H), Mori–Tanaka (M) and different ratios h/l

Fig. 6 shows the effects of the Paternak elastic foundation coefficient k_p on first three nondimensional frequencies of FGM microbeams with Winkler foundation coefficients $k_w = 50$, $n = 0.5$ and $L/h = 10$ using homogenization techniques Voigt (V), Hashin–Shtrikman (H), Mori–Tanaka (M) and different ratios $h/l = 2$ (Fig. 6(a)), $h/l = 8$ (Fig. 6(b)). It can be seen first three nondimensional frequencies increase when the foundation coefficients k_p increase. Moreover, the difference between the second frequency and the third frequency are remarkable when the ratio h/l is higher.

4. CONCLUSIONS

In this work, free vibration of FGM microbeams on the Winkler–Pasternak elastic foundation is studied based on the MCST, the TBT and Mori–Tanaka, Hashin-Shtrikman

and Voigt homogenization techniques. The differential equations of free vibration for the TBT microbeam are derived by using the FEM and Kosmatka's shape functions. The influences of the size-effect, the volume fraction index, the slenderness ratio, and foundation parameters on the first three nondimensional frequencies of the FGM microbeams were discussed in detail. The obtained numerical results allow one to make the following remarks:

- The material length scale parameter plays an important role in the frequencies of microbeams. The nondimensional frequencies decrease when the slenderness ratios h/l and the volume fraction index n increase.

- There are "turning point" ratios L/h, at which the given nondimensional frequency changes from the increase to the constant. These turning point ratios are dependent on the given frequency and the ratios h/l and L/h.

- Nondimensional frequencies using the Hashin–Shtrikman homogenization technique are a little higher than nondimensional frequencies using the Mori–Tanaka homogenization technique, but both are smaller than nondimensional frequencies using the Voigt homogenization technique, especially for the higher frequencies.

- Effects of the Winkler elastic foundation coefficients k_w on first three nondimensional frequencies of FGM microbeams are fewer than one of the Pasternak elastic foundation coefficients k_p, especially the ratio h/l is small.

All the mentioned notices are a useful indication for vibration analysis of FGM microstructures. The study can be applied to more complex microstructures.

DECLARATION OF COMPETING INTEREST

The authors declare that they have no known competing financial interests or personal relationships that could have appeared to influence the work reported in this paper.

FUNDING

This research received no specific grant from any funding agency in the public, commercial, or not-for-profit sectors.

REFERENCES

[1] F. Yang, A. C. M. Chong, D. C. C. Lam, and P. Tong. Couple stress based strain gradient theory for elasticity. *International Journal of Solids and Structures*, **39**, (2002), pp. 2731–2743. https://doi.org/10.1016/s0020-7683(02)00152-x.

[2] D. C. C. Lam, F. Yang, A. C. M. Chong, J. Wang, and P. Tong. Experiments and theory in strain gradient elasticity. *Journal of the Mechanics and Physics of Solids*, **51**, (2003), pp. 1477–1508. https://doi.org/10.1016/s0022-5096(03)00053-x.

[3] M. Şimşek and J. N. Reddy. A unified higher order beam theory for buckling of a functionally graded microbeam embedded in elastic medium using modified couple stress theory. *Composite Structures*, **101**, (2013), pp. 47–58. https://doi.org/10.1016/j.compstruct.2013.01.017.

[4] M. Şimşek and J. N. Reddy. Bending and vibration of functionally graded microbeams using a new higher order beam theory and the modified couple stress theory. *International Journal of Engineering Science*, **64**, (2013), pp. 37–53. https://doi.org/10.1016/j.ijengsci.2012.12.002.

[5] R. Ansari, R. Gholami, and S. Sahmani. Free vibration analysis of size-dependent functionally graded microbeams based on the strain gradient Timoshenko beam theory. *Composite Structures*, **94**, (2011), pp. 221–228. https://doi.org/10.1016/j.compstruct.2011.06.024.

[6] M. H. Kahrobaiyan, M. Asghari, and M. T. Ahmadian. A Timoshenko beam element based on the modified couple stress theory. *International Journal of Mechanical Sciences*, **79**, (2014), pp. 75–83. https://doi.org/10.1016/j.ijmecsci.2013.11.014.

[7] L.-L. Ke and Y.-S. Wang. Size effect on dynamic stability of functionally graded microbeams based on a modified couple stress theory. *Composite Structures*, **93**, (2011), pp. 342–350. https://doi.org/10.1016/j.compstruct.2010.09.008.

[8] H.-T. Thai, T. P. Vo, T.-K. Nguyen, and J. Lee. Size-dependent behavior of functionally graded sandwich microbeams based on the modified couple stress theory. *Composite Structures*, **123**, (2015), pp. 337–349. https://doi.org/10.1016/j.compstruct.2014.11.065.

[9] M. Salamat-talab, A. Nateghi, and J. Torabi. Static and dynamic analysis of third-order shear deformation FG micro beam based on modified couple stress theory. *International Journal of Mechanical Sciences*, **57**, (2012), pp. 63–73. https://doi.org/10.1016/j.ijmecsci.2012.02.004.

[10] B. Akgöz and Ö. Civalek. Free vibration analysis of axially functionally graded tapered Bernoulli–Euler microbeams based on the modified couple stress theory. *Composite Structures*, **98**, (2013), pp. 314–322. https://doi.org/10.1016/j.compstruct.2012.11.020.

[11] X. Chen, X. Zhang, Y. Lu, and Y. Li. Static and dynamic analysis of the postbuckling of bi-directional functionally graded material microbeams. *International Journal of Mechanical Sciences*, **151**, (2019), pp. 424–443. https://doi.org/10.1016/j.ijmecsci.2018.12.001.

[12] N. Shafiei, A. Mousavi, and M. Ghadiri. On size-dependent nonlinear vibration of porous and imperfect functionally graded tapered microbeams. *International Journal of Engineering Science*, **106**, (2016), pp. 42–56. https://doi.org/10.1016/j.ijengsci.2016.05.007.

[13] M. A. R. Loja, J. I. Barbosa, and C. M. Mota Soares. A study on the modeling of sandwich functionally graded particulate composites. *Composite Structures*, **94**, (2012), pp. 2209–2217. https://doi.org/10.1016/j.compstruct.2012.02.015.

[14] J. B. Kosmatka. An improved two-node finite element for stability and natural frequencies of axial-loaded Timoshenko beams. *Computers & Structures*, **57**, (1995), pp. 141–149. https://doi.org/10.1016/0045-7949(94)00595-t.